Available online at www.sciencedirect.com
ScienceDirect
Journal of Nuclear Materials 363–365 (2007) 1153–1159
journal of nuclear materials
www.elsevier.com/locate/jnucmat

# Surface modification at tungsten and tungsten coated graphite due to low energy and high fluence plasma and laser pulse irradiation

N. Ohno [a,*], S. Kajita [b], Dai Nishijima [b], S. Takamura [b]

[a] EcoTopia Science Institute, Nagoya University, Furo-cho, Chikusa-ku, Nagoya 464-8603, Japan
[b] Graduate School of Engineering, Nagoya University, Nagoya 464-8603, Japan

**Abstract**

We have investigated the influence of low energy helium and hydrogen/deuterium plasma irradiation to tungsten or tungsten coated graphite samples. The experimental conditions of helium hole/bubble formation and hydrogen blister formation were summarized. The tungsten coated graphite exposed to a helium plasma shows different surface modification from those of bulk tungsten. We also demonstrated a transient heat load onto a damaged tungsten surface due to a helium plasma exposure by a laser-beam irradiation. Simultaneous helium plasma and laser pulse irradiations lead to a further roughing of the tungsten surface.


*PACS:* 52.40.Hf; 52.40.−w; 52.38.Mf

*Keywords:* Tungsten; Blister; Bubble; Dust; NAGDIS-II

## 1. Introduction

Tungsten (W) is one of the most important candidates as plasma-facing materials of International Thermonuclear Experimental Reactor (ITER) because of its excellent material properties such as high melting point, high threshold energy for physical sputtering, and low retention of hydrogen isotopes. However, recent laboratory experiments revealed that helium holes/bubbles and hydrogen blisters were formed at the W with high fluence plasma irradiation even at an incident ion energies below the threshold value of physical sputtering. These experimental conditions are relevant to the high recycling divertor plasma conditions in the ITER.

First, we will summarize the hole/bubble and blister formation under a low energy and high fluence plasma exposure [1–6] in the linear divertor plasma simulator [7], including the W dust formation [8]. A low energy plasma exposure of W coated graphite was also investigated.

On the other hand, melting and evaporation of W owing to an intermittent huge heat load is anticipated

* Corresponding author. Fax: +81 52 789 3944.
*E-mail address:* ohno@ees.nagoya-u.ac.jp (N. Ohno).

0022-3115/$ - see front matter © 2007 Elsevier B.V. All rights reserved.
doi:10.1016/j.jnucmat.2007.01.148

in ITER. The hole/bubble and blister formation can cause microcracks on the W surface and strongly degrade thermal diffusivity of the W, which could lead to overheating under plasma exposure, especially high heat pulses due to ELMs. The melting of W due to the overheating strongly enhances the erosion of W. We have also demonstrated the high heat pulses to W with holes and bubbles by pulse laser irradiation.

## 2. Low energy helium and hydrogen plasma irradiation to W material

### 2.1. Helium bubble/hole and hydrogen blister formation

In this section, we will briefly summarize the experimental conditions for the helium hole/bubble and hydrogen blister formation at W in our previous works. The experiments have been carried out in the NAGDIS-II (NAGoya university DIvertor Simulator-II), which can generate high density plasma in a steady state [7]. Powder metallurgy tungsten (PM-W) samples were provided by Nilaco Co. Ltd. (Tokyo, Japan), and single crystal tungsten (SC-W) samples were used in the experiments. The thickness and purity of the PM-W samples were 0.2 mm and 99.95%, respectively.

Fig. 1 shows typical scanning electron microscope (SEM) photographs of the W exposed to a helium plasma at a surface temperature of 2200 K, an incident ion energy of 15 eV, and an ion flux of $8.3 \times 10^{22}\ m^{-2}\ s^{-1}$. It is found that a lot of holes and bubbles are formed at the W surface, and the size and the number of holes and bubbles increase with the exposure time as shown in Fig. 1(b). These helium holes and bubbles are clearly observed when the surface temperature is as large as 1300 K and the incident ion fluence is above several $10^{25}\ m^{-2}$. At a higher surface temperature, the bubble/hole formation was enhanced. The helium holes and bubbles were also generated at the SC-W, which indicates that the intrinsic defects have little effect on the hole/bubble formation. At present, it is concluded that the key physics of the helium hole/bubble formation is trapping of helium atoms to thermal vacancies generated at a high surface temperature.

The large blisters (above 10 μm) were formed on the PM-W irradiated by hydrogen/deuterium plasmas at a surface temperature below 900 K (Fig. 2(a)). It is found from the cross section of the blister as shown in Fig. 2(b) that the large blister is formed by cleaving along the stratified layer especially in the cold-worked PM-W samples. There were no blisters formed at the hot-worked PM-W and the SC-W. On the other hand, recent studies reported that small blisters (2 μm) were formed even at hot-worked PM-W and SC-W by a deuterium plasma irradiation [9,10], although we have not yet observed such small blisters. In Ref. [10], it was indicated that the maximum diameter of the blisters was about 2–3 μm. The formation of small blisters was discussed based on oxide layer formation at the W surface.

### 2.2. W dust formation

Various kinds of dust particles have been observed in fusion devices. The dust formation would have strong influence on a plasma perfor-

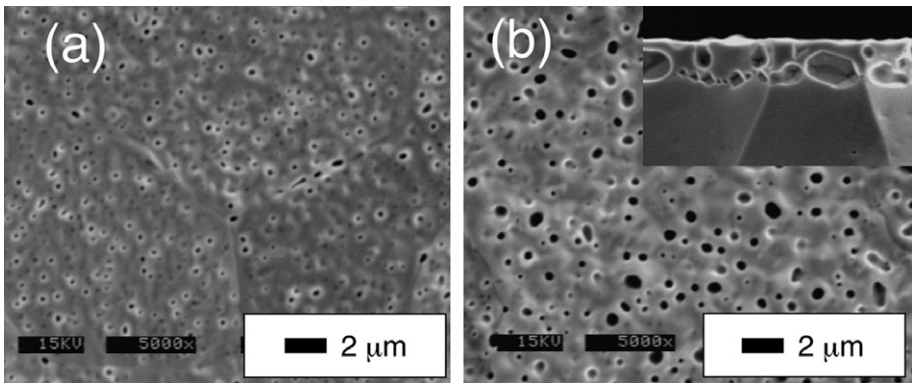


Fig. 1. SEM photographs showing the helium hole and bubble formation on a powder metallurgy tungsten sample irradiated by a helium plasma at a surface temperature of 2200 K with an incident ion energy of 15 eV and an ion flux of $8.3 \times 10^{22}\ m^{-2}\ s^{-1}$. The exposure time is (a) 1000 s and (b) 10000 s, respectively. The cross section of (b) is shown in the inset.

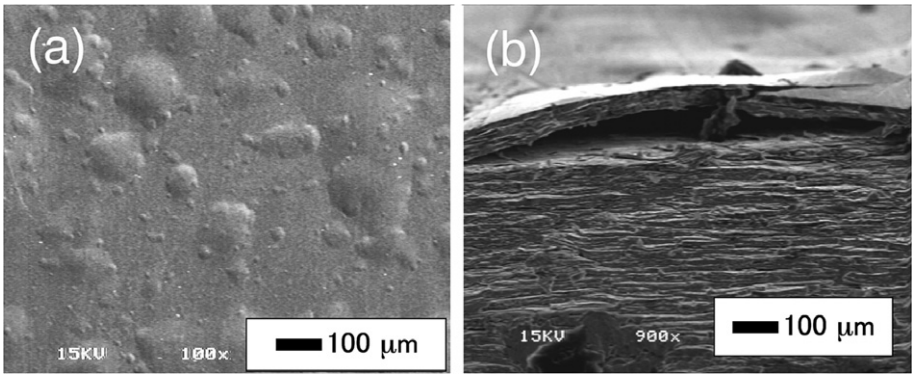


Fig. 2. SEM photographs of blisters on a powder metallurgy tungsten sample exposed to a hydrogen plasma at 550 K. The ion incident energy and the fluence are 90 eV and $3.4 \times 10^{25}$ m$^{-2}$, respectively; (b) is a cross section of (a).

mance. Especially, high $Z$ dust particles become huge impurities. Our recent observation shows that there are two types of the dust generation from the W. Fig. 3(a) shows the SEM image of W exposed to a deuterium plasma. Blister exfoliations were observed and the exfoliated W blisters become the high $Z$ dust particles. The dust particles are mainly generated from the small blisters. At present, we cannot understand why the small blisters can be exfoliated much more easily than the larger ones.

Fig. 3(b) shows the ejected grain particles from the W sample with helium holes and bubbles. The sample was irradiated by a deuterium plasma at 550 K subsequent to the helium plasma pre-exposure at 1600 K. The helium bubbles formed along the grain boundary could make grain ejection much easier.

### 2.3. Helium and deuterium plasma exposure of W coated graphite

W coated graphite, which could overcome the disadvantages of tungsten such as heavy weight and poor workability, were recently used as plasma-facing components in some fusion devices [11–14]. Various kinds of W coated materials have been manufactured by plasma spaying (PS), physical vapor deposition (PVD), and chemical vapor deposition (CVD) [15,16]. Thick W coating on the graphite, having good thermal and adhesion properties, can be made by the PS technique. Although the W coated graphite has been tested under a high heat load by using an electron beam, there are few experiments on the helium and hydrogen plasma irradiation to the W coated graphite.

The fine-grained graphite IG-430U (Toyo Tanso Co.) substrate, 20 mm × 20 mm × 10 mm, was coated with W using the PS technique (PS-W). The thickness of the PS-W layer is 1.0 mm. The rhenium layers exist between the PS-W layer and the fine-grained graphite as a diffusion barrier layer. Fig. 4(a) shows the SEM photograph of the PS-W coated graphite surface before plasma irradiation. Several tungsten layers were overlapped each other. The sample was then exposed by a helium plasma at 1600 K, an ion fluence of $3.7 \times 10^{27}$ m$^{-2}$ and an ion

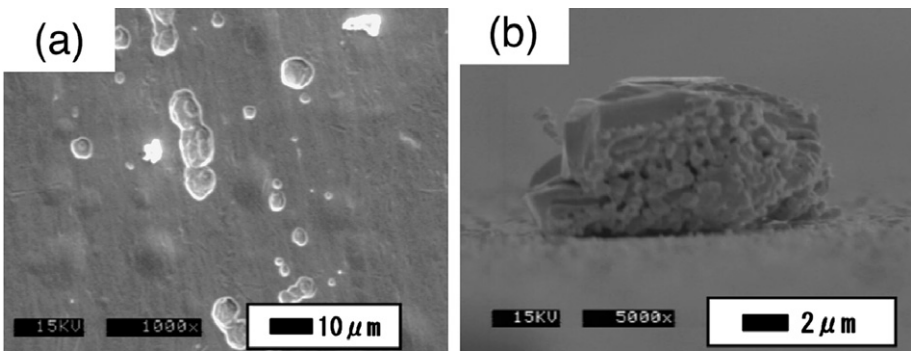


Fig. 3. SEM photographs of tungsten dust formation: (a) hydrogen blisters with a diameter less than 10 μm are exfoliated, (b) tungsten grain ejection from the tungsten surface deuterium plasma exposure at 550 K, subsequent helium plasma exposure at 1600 K.

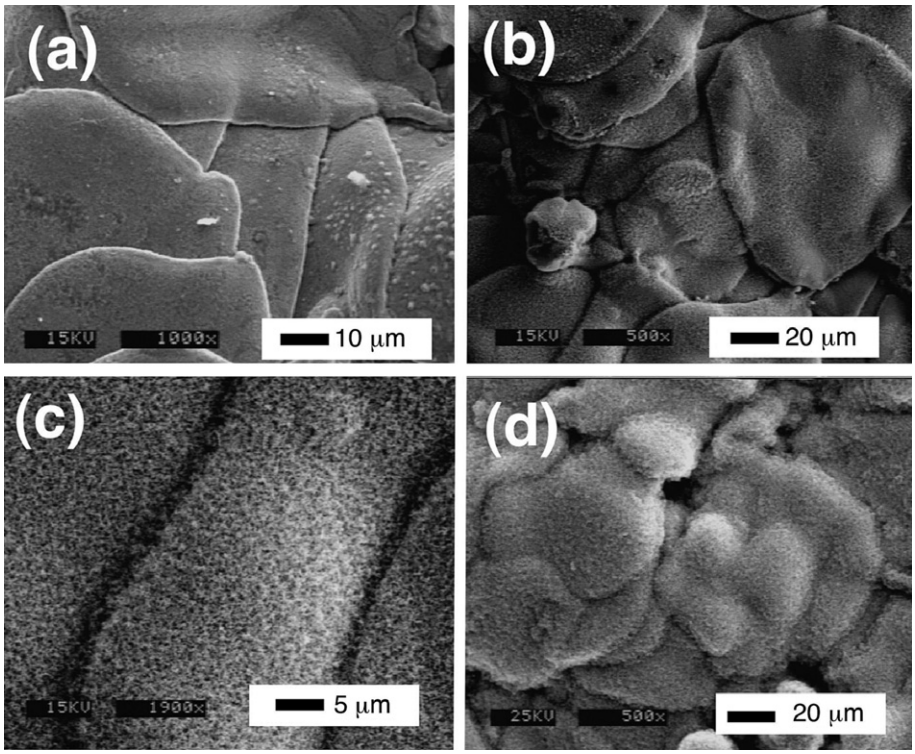


Fig. 4. SEM photographs of tungsten coated graphite samples made by a plasma spray coating method, (a) as received, (b) exposed to a helium plasma at 1600 K with an ion incident energy of 12.5 eV and an ion fluence of $3.4 \times 10^{27}$ m$^{-2}$, respectively, (c) enlargement of (b), and (d) at 1250 K with an ion incident energy of 11.3 eV and an ion fluence of $3.5 \times 10^{27}$ m$^{-2}$, respectively.

incident energy of 12.5 eV. These experimental parameters correspond to the conditions for helium bubble and hole generation at the PM-W and the SC-W as mentioned before, however, no micron-sized holes were observed in Fig. 4(b). On the other hand, the surface was covered by a submicron fine structure, resulting in blacking of the surface as shown in Fig. 4(c), which is the enlargement of Fig. 4(b). At a lower surface temperature ~1250 K, the fine structure covering the surface becomes much thicker (Fig. 4(d)), leading to no visible light reflection on the surface. EDX analysis shows that the fine structure is made of W.

The PS-W coated graphite was also irradiated by a deuterium plasma at 600 K. There were no large blisters with a diameter of more than 10 μm at the PS-W surface, although the large blisters were observed at the PM-W surface in the same experimental condition corresponding to Fig. 2. A recent study indicated that very small blisters (about 0.2 μm) were observed at the surface of PS-W coated graphite [9]. Unfortunately, we could not observe such small blisters because of the poor spatial resolution of the SEM analysis.

The PS-W coated graphite shows the different properties compared with the PM-W and the SC-W.

## 3. Transient heat load to tungsten samples irradiated by laser

The transient heat load to the W samples being exposed to helium plasmas was demonstrated using pulsed laser irradiation [17]. The helium plasma was irradiated to PM-W samples suited at about 45° inclined to the magnetic line of force. Second harmonic pulses of an Nd:YAG laser with a wavelength of 532 nm, were used. Fig. 5(a) and (b) shows SEM photographs of the PM-W samples exposed to a helium plasma without and with simultaneous laser pulses (18 000 pulses), respectively. The incident energy and fluence of the helium ion were 27 eV and $4.9 \times 10^{28}$ m$^{-2}$, respectively. The pulse duration was 5–7 ns, and the pulse interval was 0.1 s. The laser pulse energy was 200 mJ/cm$^2$. The surface temperature of the PM-W sample during He plasma irradiation was 1700 K without the laser pulses. The temporal evolution of the surface temperature during the laser pulse irradiation could

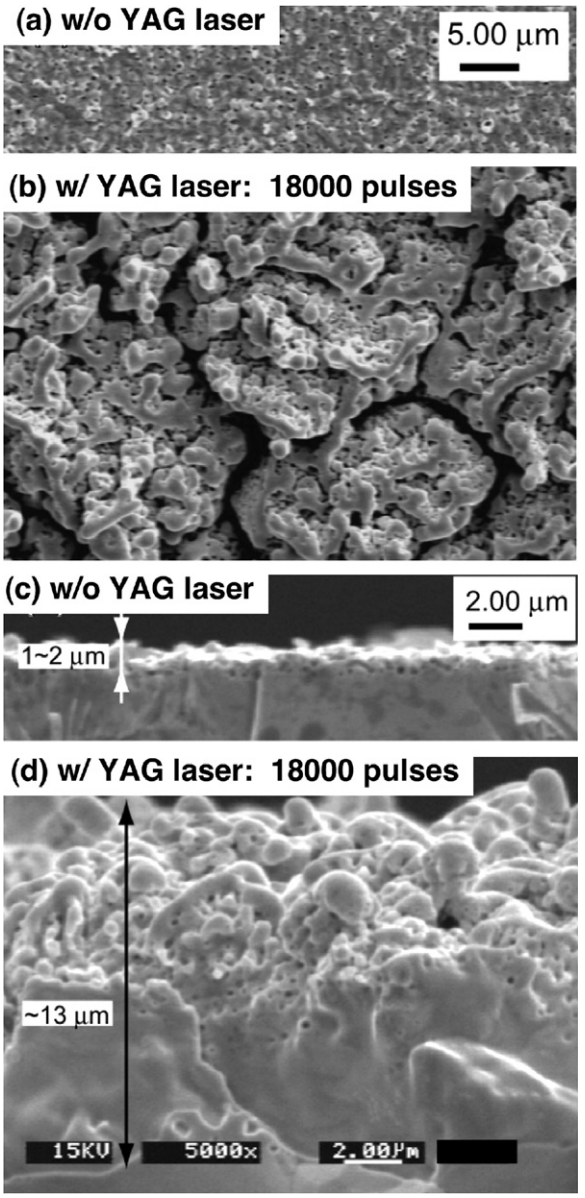


Fig. 5. SEM photographs of surface of powder metallurgy tungsten (a) without YAG laser irradiation, (b) with YAG laser irradiation during helium plasma exposure, (c) and (d) is the cross sections of (a) and (b), respectively.

not be measured. It is found that the size of the bubbles and holes formed with the laser pulses became much larger than those without the laser pulses, and the penetration depth of bubbles was 13 μm as shown in Fig. 5(d), which is much deeper than that without the laser irradiation (Fig. 5(c)). We observed the PM-W surface irradiated by the 18 000 laser pulses with the laser pulse energy of 600 mJ/cm$^2$ without helium plasma irradiation in vacuum. By taking account of the light reflectivity at the W surface without helium plasma irradiation, the absorbed energy can be estimated to about 60% of the laser output energy [18]. Although the absorbed energy in vacuum with a laser pulse energy of 600 mJ/cm$^2$ is about twice as large as that shown in Fig. 5(a), the surface modification with a depth of ~10 μm was not observed.

We analytically estimated the surface temperature change in response to the laser pulse [19,20]. The surface temperature rise due to heating by a temporal triangle-shaped laser pulse with an absorbed energy of 200 mJ/cm$^2$ having the raising time of 3.5 ns and falling time of 3.5 ns can be estimated to be 1380 K by using thermal conductivity (174 W/m K), specific heat capacity (138 J/kg K), and density (19 000 kg/m$^3$) for the bulk W. Thus, the maximum surface temperature reaches about 3100 K in the experiment, which is lower than the melting point of W. However, when the holes and bubbles are formed in W, we need to consider three-dimensional heat transfer by taking the effect of holes and bubbles into account because the characteristic depth of the heat transfer during the laser pulse duration is 1 μm, which is comparable of the characteristic depth of the surface modification due to the helium plasma irradiation. We developed a three-dimensional heat transfer model taking the effect of helium holes into account. The model calculation shows that the surface temperature can heat up locally to reach the melting temperature of W due to the laser pulse even at 200 mJ/cm$^2$ [21].

The laser pulses were also irradiated to the PM-W surface with a helium hole and a bubble structure in vacuum. The surface roughness was enhanced in comparison with the PM-W irradiated by the same laser pulses in vacuum, which indicates that the effective thermal diffusivity is considerably reduced due to the formation of the bubbles and holes at the surface. On the other hand, the surface roughness of the PM-W surface depicted in Fig. 5(b), irradiated by a helium plasma and laser pulses simultaneously, is much larger than that of the laser irradiated PM-W surface with holes and bubbles in vacuum, indicating that the simultaneous helium plasma and laser pulse irradiations to PM-W lead to a further roughing of the PM-W surface. Thin W layer between the helium bubble and the W surface could be melt by the local overheating due to the laser pulse. New rough W surface appears and helium bubbles are formed again at the deeper region of W. Such surface change is repeated to

induce a deeper modification in the case of simultaneous helium plasma and laser pulse irradiation. So-called synergetic effect works if a helium plasma irradiation and a transient heat pulse to the PM-W surface exist simultaneously.

The YAG laser pulse duration is several ns, which is much shorter than the characteristic time of the ELMs (1 ms). Thus, the ruby laser without Q switch was employed to generate the laser pulse with a duration of 0.5 ms and a wavelength of 694 nm. The heat flux is 6–10 J/cm$^2$. Ten ruby laser pulses were irradiated to the PS-W coated graphite sample with the submicron fine structure, corresponding to Fig. 4(c). A lot of W droplets due to the melting of the PS-W surface were observed as shown in Fig. 6(a). Fig. 6(b) shows the time evolution of the surface temperature calculated by a one-dimensional heat equation. In this calculation, the laser heat flux is 10 J/cm$^2$, and the shape of the laser pulse is a triangular temporal evolution having the rising time and the falling time of 0.5 ms for each pulse. As the thermal diffusivity of bulk tungsten is assumed, the temperature rise is only 200 K, indicated as 100% in the figure. In order to reach the melting point of W, the thermal diffusivity should be reduced to be 1% of the bulk value. This calculation indicates that the thermal diffusivity is dramatically degraded for the W fine structure shown in Fig. 4(c).

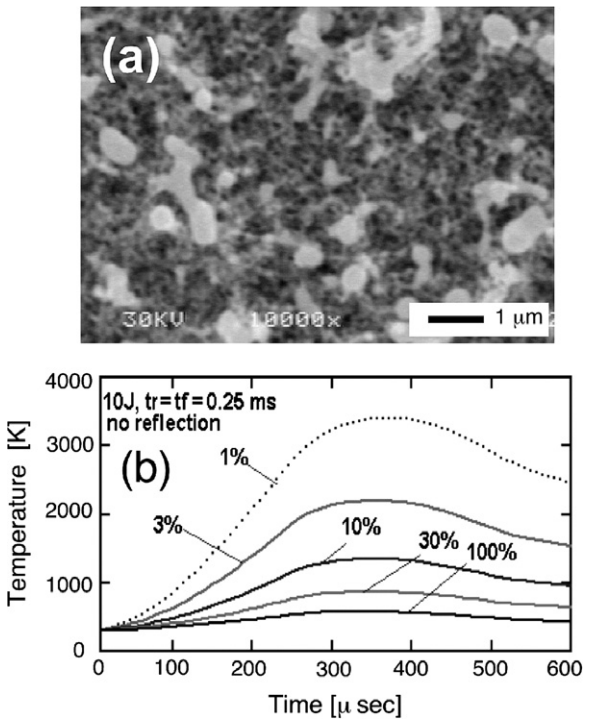


Fig. 6. (a) SEM photograph of tungsten coated graphite surface of Fig. 4(c) after ruby laser irradiation. (b) Time evolution of the surface temperature calculated by a one-dimensional heat diffusion equation by taking into account of the degradation of thermal diffusivity.

## 4. Conclusions

Low energy helium and hydrogen/deuterium plasma irradiations to the W and W coated graphite have been investigated using the linear divertor plasma simulator NAGDIS-II. The holes and bubbles were generated under the conditions of the W surface temperature $T > 1300$ K and fluence $> 10^{25}$–$10^{26}$ m$^{-2}$, and large hydrogen blisters (more than 10 μm) at $T < 900$ K and fluence $> 10^{25}$–$10^{26}$ m$^{-2}$. The W dust was generated from exfoliation of small H blisters below 10 μm in diameter, and also from the ejected W grains. The W coated graphite was also tested, which shows different features from the bulk W. The transient heat load by laser pulses is irradiated to the W surfaces with hole/bubble structure and/or W fine structure. The surface modification degrades the thermal diffusivity of the W, leading to the enhancement of the surface roughness and melting of the W surface.

## Acknowledgements

We wish to thank Professor N. Yoshida, Dr. K. Tokunaga of the Kyushu University, Professor N. Noda of NIFS for providing the W coated graphite sample and a fruitful discussion, and Mr. M. Takagi of the Nagoya University for his excellent technical support.

## References

[1] M.Y. Ye, S. Fukuta, N. Ohno, et al., J. Plasma Fusion Res. 3 (2000) 265.
[2] M.Y. Ye, H. Kanehara, S. Fukuta, et al., J. Nucl. Mater. 313–316 (2003) 72.
[3] D. Nishijima, M.Y. Ye, N. Ohno, et al., J. Nucl. Mater. 329–333 (2004) 1029.
[4] D. Nishijima, T. Sugimoto, M. Ye, et al., Jpn. J. Appl. Phys. 44 (2005) 380.
[5] D. Nishijima, H. Iwakiri, K. Amano, et al., Nucl. Fusion 45 (2005) 669.
[6] D. Nishijima, T. Sugimoto, H. Iwakiri, et al., J. Nucl. Mater. 337–339 (2005) 927.
[7] N. Ohno, D. Nishijima, S. Takamura, et al., Nucl. Fusion 41 (2001) 1055.

[8] D. Nishijima, K. Amano, N. Ohno, et al., J. Plasma Fusion Res. 81 (2005) 703.
[9] K. Tokunaga, M.J. Baldwin, R.P. Doerner, et al., J. Nucl. Mater. 337–339 (2005) 887.
[10] G.-N. Luo, W.M. Shu, M. Nishi, J. Nucl. Mater. 347 (2005) 111.
[11] A. Tabasso, H. Maiser, K. Krieger, et al., Nucl. Fusion 40 (2000) 1441.
[12] H. Maier, J. Luthin, M. Balden, et al., J. Nucl. Mater. 307–311 (2002) 116.
[13] R. Neu, R. Dux, A. Geier, et al., J. Nucl. Mater. 313–316 (2003) 116.
[14] H. Maier, ASDEX Upgrade Team, J. Nucl. Mater. 335 (2004) 515.
[15] K. Tokunaga, N. Yoshida, N. Noda, et al., J. Nucl. Mater. 266–269 (1999) 1224.
[16] K. Tokunaga, T. Matsubara, Y. Miyamoto, et al., J. Nucl. Mater. 283–287 (2000) 1121.
[17] S. Kajita, D. Nishijima, N. Ohno, et al., J. Plasma Fusion Res. 81 (2005) 745.
[18] M. Ye, S. Fukuta, N. Ohno, S. Takamura, K. Tokunaga, N. Yoshida, J. Plasma Fusion Res. SERIES 3 (2000) 265.
[19] Jui-Teng Lin, Thomas F. George, J. Appl. Phys. 54 (1983) 382.
[20] D. Burgess, P.C. Stair, E. Weitz, J. Vac. Sci. Technol. A 4 (1986) 1362.
[21] S. Kajita, Dai Nishijima, N. Ohno, S. Takamura, J. Appl. Phys. 100 (2006) 103304.